BS 2023 4-6 SEPT SHANGHAI
International Building Performance Simulation Association

A novel rooftop solar energy potential estimation method based on deep learning at district level

Guannan Li[1,2,3], Zixi Wang[1,2], Chengliang Xu[1,2]
[1]School of Urban Construction, Wuhan University of Science and Technology, Wuhan 430065, China
[2]Hubei Provincial Engineering Research Center of Urban Regeneration, Wuhan University of Science and Technology, Wuhan 430065, China
[3]State Key Laboratory of Green Building in Western China, Xi'an University of Architecture & Technology, Xi'an 710055, China

Abstract

Accurate assessment of rooftop solar potential is becoming increasingly important in sustainable urban development. Due to the different uses of urban roof buildings, it is difficult to accurately estimate the availability of roofs to solar radiation. To address this challenge, this study proposed a framework for estimating the rooftop solar potential at the district level by integrating deep leaning and geographic information system (GIS).

To verify the methodology, a district in Wuhan that contains a variety of building features was used. The results show that classifying roofs by building type can effectively improve the accuracy of identifying roof availability. The integrated approach proposed in this work offers reference means for assessing the solar potential of district building rooftops.

Highlights

- High-precision assessment of urban roof solar potential based on U^2-Net.
- Consider the effect of roof obstacles on the available roof area.
- Verify the calculation by combining the solar radiation simulation.

Introduction

The application of renewable energy is crucial for urban decarbonization. China clearly proposes to reach a carbon peak by 2030 and strive for carbon neutrality by 2060. The "14th Five-Year Plan" and the 2035 Vision Target Outline adopted by the NPC and CPPCC have set clear requirements for the development of renewable energy.

Due to the huge energy consumption in existing cities, the efficient use of renewable energy has become increasingly crucial. Therefore, urban rooftop solar photovoltaic integration is an effective method to solve urban energy demands. As a basic prerequisite, accurate assessment of rooftop solar potential is becoming increasingly important in urban sustainable development. To estimate the solar photovoltaic potential of urban rooftops, it is necessary to quantify the available rooftop area of buildings that can receive solar radiation.

A large amount of open data from public map service projects is used to evaluate urban planning(Liang, Gong, and Li 2018). For example, as an open data source, Google Earth Satellite (GES) images have the advantages of wide coverage and fast update speed(Qi and Wang 2014). In recent years, with the help of abundant data sets, the emerging image semantic segmentation method based on deep learning has achieved relatively satisfactory results in building rooftop recognition and rooftop photovoltaic panel recognition. Deep learning provides methodological support for extracting information related to urban rooftops(Shi, Li, and Zhu 2020), and further contributes to estimating the solar potential of urban rooftops (Huang, Mendis, and Xu 2019).

In recent years, deep learning especially the deep convolutional neural network (CNN) has been widely used in image recognition and classification task. As the network architecture becomes more and more in-depth and extensive, VGGNet achieved the most advanced results successfully in 2014 (K and A 2014). As one of the most advanced deep learning technologies at present, the U-Net model, whose basic framework was first proposed (O, P, and T 2015) in 2015, aims to solve the problem of image segmentation. The network can be trained to obtain high-precision results with fewer data sets(V 2018). Qin et al.(Qin et al. 2020) built a U^2-Net with a two-layer nested U-shaped structure, and increase the depth of the entire architecture without significantly increasing computing costs.

In the field of potential evaluation of rooftop solar PV, many scholars have conducted relevant research. Zhong et al. (Zhong et al. 2021) proposed an automatic extraction method for rooftops based on deep learning. The model is trained by taking part of Nanjing as an example and the overall accuracy of the extracted roof reached 0.92. Huang et al.(Huang, Mendis, and Xu 2019) used U-Net and a number of satellite maps to identify building rooftops to further estimate the solar potential of city. The results establish that the annual photovoltaic generation potential of urban rooftop in Wuhan is 17292.30 × 106 kW·h/year. Dixit et al.(Dixit, Chaurasia, and Kumar Mishra 2021) developed a ResUnet-based deep learning for building contour recognition using 10 m resolution multispectral satellite images.

However, the rooftop area extracted directly does not

https://doi.org/10.26868/25222708.2023.1450

necessarily equal the available area of the building rooftop. The solar potential of rooftops is greatly overestimated by obstacles that often affect the available area of rooftops. To mitigate the impact of rooftop obstacles, some studies consider using rooftop availability factors to simulate the impact of rooftop obstacles. Zhang et al.(Zhang et al. 2021) constructed a workflow based on deep learning, in which different rooftops can be estimated using utilization coefficients according to different land use types. Due to the different construction styles and different uses of buildings, the distribution and construction of building rooftop obstacles are irregular. Therefore, only using the rooftop availability factor to evaluate tends to result in large errors. Ren et al.(Ren et al. 2022) proposed a new integration method of 3D-Geographic Information System (GIS) and deep learning, which takes into account both the shading effect of buildings and the rooftop obstacles. The results display that the annual solar potential of the entire building community has been reduced by 35.7% due to the shading effect and the reduced rooftop availability. Yu et al. (Yu et al. 2018) developed an accurate deep learning framework that automatically locates and estimates the size of solar photovoltaic panels from satellite images.

In summary, it is difficult to assess solar potential of high-density urban rooftops more comprehensively in existing studies, mainly because the results are not ideal in complex rooftop situations (Mainzer et al. 2017), and the identification of rooftop obstacles according to different building types is not considered (Ren et al. 2022).

To solve the above problems, this paper uses U^2-Net model for image semantics segmentation based on deep learning, aiming at the following two aspects:

(1) Take an area in Wuhan that contains a variety of building features as an example, and obtain training models of data sets according to "industry", "commercial", "residence". Based on the direct training model without classification, this paper explores the impact of building type classification on the prediction results.

(2) Both rooftop and rooftop obstacle identification are considered, and the identification accuracy is considered to improve the accuracy of rooftop available area assessment. The solar potential is evaluated with the calculated solar radiation in Wuhan.

Description of methods and data

Figure 1 illustrates an integrated approach of QGIS and deep learning for urban high-precision rooftop solar potential assessment. It mainly consists of two parts, combined with solar radiation intensity simulation analysis and a deep learning framework for roof availability identification. For roof identification, the deep learning framework uses satellite imagery as input. In this frame, U2-Net model is used to identify the rooftop and obstacles respectively, and then the area of obstacles is subtracted from the total area of the roof to get the available area of the roof.

For the simulation analysis of solar radiation intensity, the dynamic solar irradiance was calculated using the RayMan irradiance model, and combined with the calculated available roof area, to complete the evaluation of rooftop solar potential in urban areas.

The construction method of this paper is introduced in Figure 2, which mainly includes four parts: (1) Data preparation, (2) Classification of building types, (3) Comparison of results, (4) Solar potential estimation.

(1) Data preparation: mainly including the acquisition of raw data and the production of label image data. The original satellite image comes from the Google satellite imagery map. Using QGIS to visualize the distribution of major land use types in Wuhan, this paper combines vector data from the open-source data website OSM (Open Street Map). Manually label the corresponding "rooftop" and "obstacle" by labelme, as seen in Figure 3. Setting the picture resolution to 2000 × 2000, actual size is 100 × 100 m when using QGIS to export satellite images.

(2) Classification of building types: Based on the type of land use, satellite images and corresponding label data are obtained for the three major types of buildings: "commercial", "industry", and "residence".. Table 1 shows the selection of data quantities for various types of buildings. The training and testing datasets of the images are randomly extracted, while the strict correspondence between the satellite images and their labels is guaranteed. Unclassified and classified test data remain the same. It is worth noting that classification refers to dividing image data into three types of buildings and calculating them separately， Unclassified refers to the direct use of all image data for calculation.

Table 1: The selection of data quantities for various types of buildings.

Building Type	Classified		Unclassified	
	Train data	Test data	Train data	Test data
Commercial	47	10	326	10
Industry	107	26		26
Residence	172	40		40

(3) Comparison of results: For the labels of "rooftop" and "obstacle", compare the predicted results of classified and unclassified building types through evaluation indicators, and explore the impact of classified processing on the identification results.

(4) Solar potential estimation: calculate the available area of the rooftop based on the identification results of the rooftop and obstacles, and evaluate the solar potential of the rooftop using the solar radiation amount calculated by the RayMan model(Matzarakis, Rutz, and Mayer 2010).

https://doi.org/10.26868/25222708.2023.1450

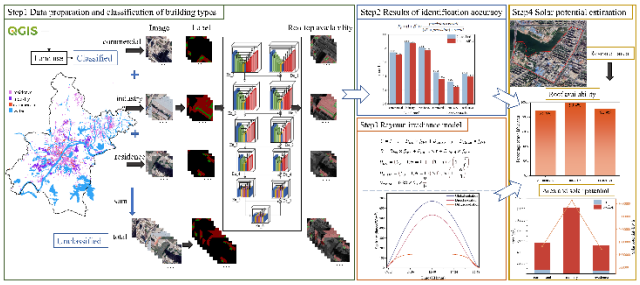

Figure 1：Illustration of the research process

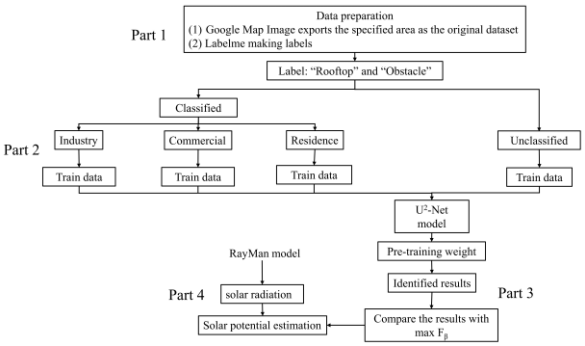

Figure 2: Research framework

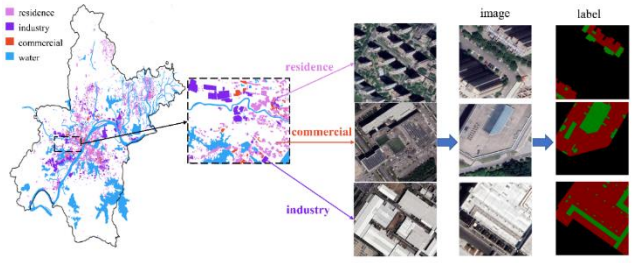

Figure 3: Acquisition process of image and label data

Construction of the U²-Net model

As shown in Figure 4, U²-Net is mainly composed of three parts(Qin et al. 2020): (1) a six segment encoder, (2) a five segment decoder, and (3) a salient image fusion module connected to the decoder level and the last segment encoder.

The working principle is as follows: First, collect the output of De_ 1, De_ 2, De_ 3, De_ 4, De_ 5 and En_6 to obtain a feature map with a channel of 1 through a 3 × 3 convolution layer, and then scaled to the size of the input image through bilinear interpolation to obtain Sup1, Sup2, Sup3, Sup4, Sup5, and Sup6. Next, these six feature maps are jointed by Concat. Finally, the final prediction probability map is obtained through a 1 × 1 convolution layer and a Sigmoid activation function.

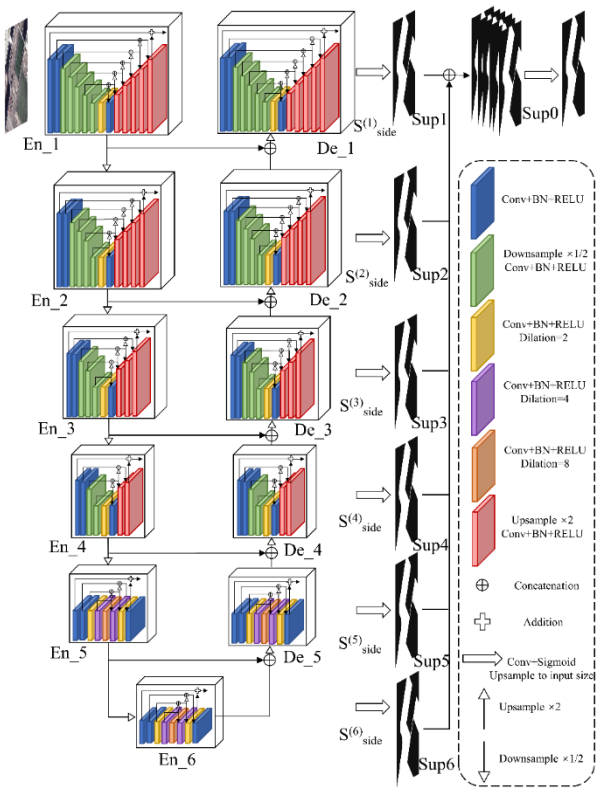

Figure 4: Structure of U²-Net model

Evaluating indicator

To take into account the impact of both accuracy and recall, this paper takes $maxF_\beta$ as an evaluation indicator to measure the prediction of the results.

F-measure F_β is used for comprehensive evaluation of precision and recall, as shown in Eq. (1):

$$F_\beta = \frac{(1+\beta^2) \times Precision \times Recall}{\beta^2 \times Precision + Recall} \quad (1)$$

Where β^2 takes 0.3(Liu, Han, and Yang 2018; Zhang et al. 2018) and report the maximum F_β ($maxF_\beta$) for each dataset.

Calculation of solar radiation on rooftops

The RayMan model is used to calculate the amount of solar radiation on the rooftop. The total horizontal solar radiation on the rooftop can be determined using equations, which are mainly calculated from the sum of direct and scattered solar radiation I and D, as shown in Eq. (2) and Eq. (3). The variable f is a binary variable that indicates whether a given point on the rooftop is obscured by any other building. If the given point is obscured, it is 0, otherwise it is 1 (this paper assumes that the rooftop is not obscured by other objects, and it is set to 1). Sky angle of view factor f_{SVF} represents the ratio of the visible sky observed from a point to the entire sky hemisphere centered at a given location.

$$G = I \times f + D_{iso} \times f_{SVF} + D_{aniso} \times f + D_{cloud} \times f_{SVF} \quad (2)$$

$$D = D_{iso} \times f_{SVF} + D_{aniso} \times f + D_{cloud} \times f_{SVF} \quad (3)$$

Where G is the total horizontal solar irradiance, I is the direct horizontal irradiance, f is a binary indicator of shadow, and f_{SVF} is the sky angle factor, D_{iso}, D_{aniso}, D_{Cloud} is the isotropic component, anisotropic component, and overcast component of diffuse solar irradiance without shadows.

Using the RayMan model, the full day solar irradiance on the rooftop is calculated based on solar irradiance data provided by the observatory or typical meteorological year weather data. The calculation of isotropic component, anisotropic component, and overcast component is shown in Eq. (4) to Eq. (6).

$$D_{iso} = \left(G_0 - \mathrm{I}(N=0)\right) \times (1-\tau) \times \left(1 - \frac{N}{8}\right) \quad (4)$$

$$D_{aniso} = \left(G_0 - \mathrm{I}(N=0)\right) \times (\tau) \times \left(1 - \frac{N}{8}\right) \quad (5)$$

$$D_{cloud} = 0.28 \times G_0 \times \frac{N}{8} \quad (6)$$

Where G_0 is the global irradiance without shadows or clouds, and I (N=0) is the direct irradiance without shadows or clouds, τ is the transmittance of direct solar radiation, and N is the amount of cloud in units of one eighth.

Results and Discussion

Identification results of rooftops and obstacles of different types of buildings

Due to different building uses often having different rooftop structures, there may be significant differences in the structure and distribution of obstacles for different types of buildings. To explore the results of rooftop and obstacle identification for different types of buildings, each training model was iterated 500 epochs, taking $maxF_\beta$ compare the identification results for evaluation indicators.

For commercial buildings with less training data, as components such as air conditioning units are often placed on the rooftops of commercial buildings, the proportion of obstacles in commercial buildings is usually large. As shown in Figure 5, when the identification label is "rooftop", $maxF_\beta$ is still in a fluctuating trend after the iteration, and the difference between the classified and unclassified recognition results is small, and both are below 0.8. For the "obstacle" label, the $maxF_\beta$ under classification processing 0.454 after the iteration, significantly higher than the unclassified $maxF_\beta$ (0.364).

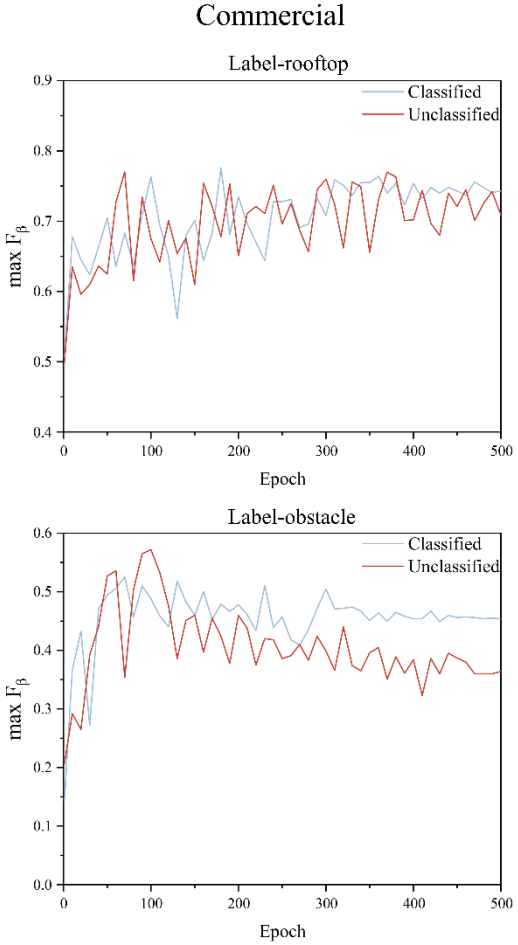

Figure 5: Identification results of commercial buildings

The main characteristics of industrial buildings are that the rooftop area is large and there are fewer obstacles. This characteristic results in a large amount of training data for the "rooftop" label and a small amount of training data for the "obstacle" label for industrial buildings. In Figure 6, when the identification label is "rooftop", after the model iteration, the change trend of classification and unclassified $maxF_\beta$ is approximately the same, both approaching 0.9, and the recognition effect after classification processing is relatively good. When the identification label is "obstacle", the value of $maxF_\beta$ after classification is significantly higher than that obtained without classification. The value of $maxF_\beta$ after classification reaches 0.32, while the value of $maxF_\beta$ without treatment is only around 0.26. This indicates that the recognition of $maxF_\beta$ after classification processing has been improved to a certain extent, and the recognition effect is better than that of unclassified $maxF_\beta$.

https://doi.org/10.26868/25222708.2023.1450

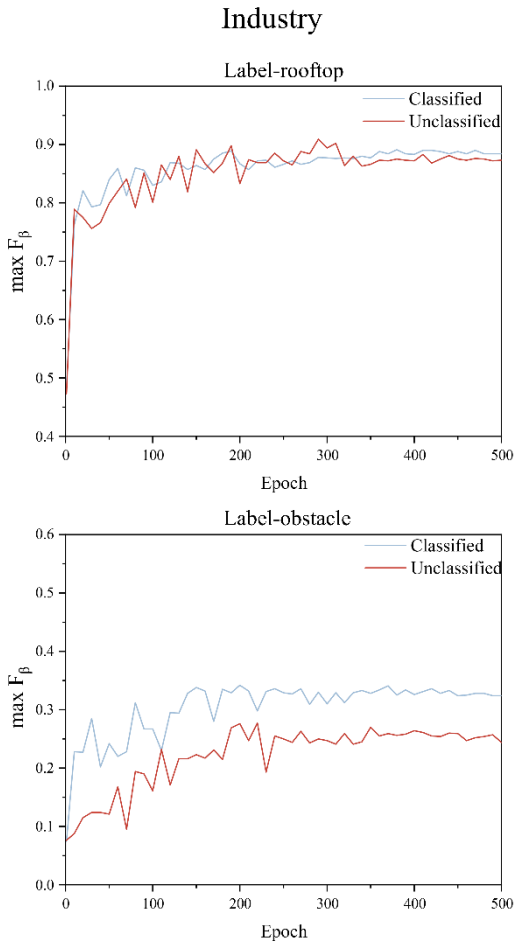

Figure 6: Identification results of industrial buildings

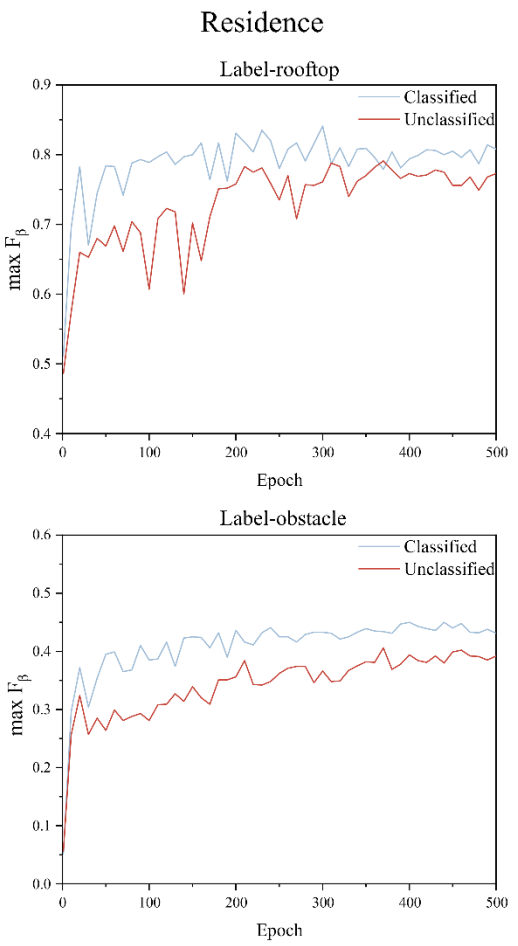

Figure 7: Identification results of residential buildings

There are significant differences in residential buildings styles in different regions, which have a certain impact on the proportion of obstacles. Generally, the proportion of obstacles in residential buildings is lower than that of commercial buildings, and higher than that of industrial buildings. In residential buildings, the identification results of labels "rooftop" and "obstacle" are shown as follows: on the overall trend, the $maxF_\beta$ value after classification processing is relatively higher, and the identification results are relatively better. For the label "rooftop", after the iteration, the classified $maxF_\beta$ value reached 0.808, higher than the unclassified $maxF_\beta$ value of 0.773. For the label "obstacle", after the iteration, the classified $maxF_\beta$ value reached 0.431, higher than the unclassified $maxF_\beta$ value of 0.392.

Impact of building classification processing on identification results

To further clarify the impact of building classification processing on the identification results, the final results of 500 epochs were taken for each type of label for each type of building, as displayed in Figure 8. Overall, the $maxF_\beta$ after classification is higher than that without classification. The value of the identification result $maxF_\beta$ for the label "rooftop" is much higher than for the "obstacle", which means that there is a more accurate identification result for the rooftop. When the label is "rooftop", the $maxF_\beta$ of industrial buildings is relatively higher, with a calculated $maxF_\beta$ of 0.884 after classification, while the $maxF_\beta$ of commercial buildings is the lowest, with a calculated $maxF_\beta$ of 0.743 after classification, which means that the rooftop recognition effect of industrial buildings is better. When the label is "obstacle", the $maxF_\beta$ difference between classified and unclassified treatment is relatively more significant. Among them, for industrial buildings with fewer "obstacle" labels, the value of $maxF_\beta$ is the lowest, and after classification, the calculated value of $maxF_\beta$ is only 0.324, with the worst recognition effect.

https://doi.org/10.26868/25222708.2023.1450

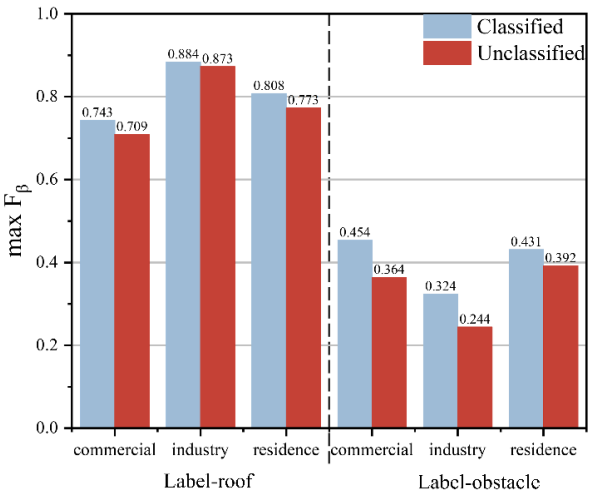

Figure 8: Results of three types of building identification

Simulation results of roof solar irradiance

The total horizontal solar radiation, direct solar radiation, and scattered solar radiation on the rooftop are simulated using the RayMan model, and the results are shown in Figure 9. Taking a typical heating day in Wuhan as an example, the variation of each radiation amount during this day is displayed. Based on the simulation results of solar irradiance, the daily solar radiation is integrated. Based on the available area of roofs of various buildings, the solar potential of the designated area can be calculated, and the results are as follows:

(1) Commercial: 25.621 kW·h/m^2 × 51744.1925 m^2 = 1325737.956 kW·h

(2) Industry: 25.621 kW·h/m^2 × 122513.8825 m^2 = 3138928.184 kW·h

(3) Residence: 25.621 kW·h/m^2 × 47511.3325 m^2 = 1217287.85 kW·h

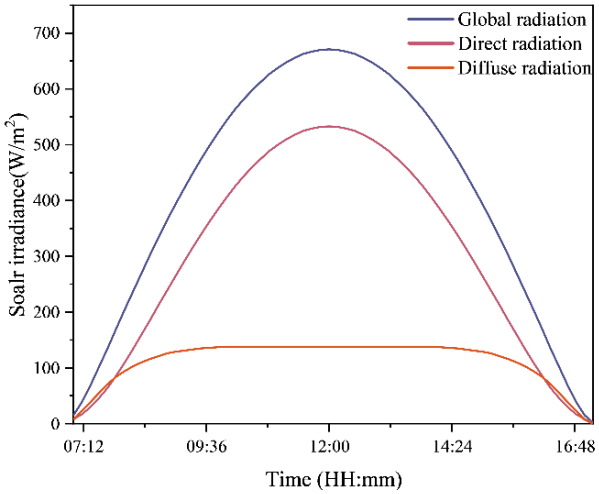

Figure 9: Simulated calculation results of solar irradiance

The study was carried out in an area of Hanyang District, Wuhan, as shown in Figure 10. The recognition results of the three types of building training sets after classification processing are established in Figure 11. Obviously, the proportion of rooftop obstacle area in industrial buildings is very small, that is, the maximum available rooftop area is 123227.08 m^2, while the obstacle area is only 713.20 m^2. For commercial buildings, the proportion of roof obstacle area is relatively high.

Figure 10: study area

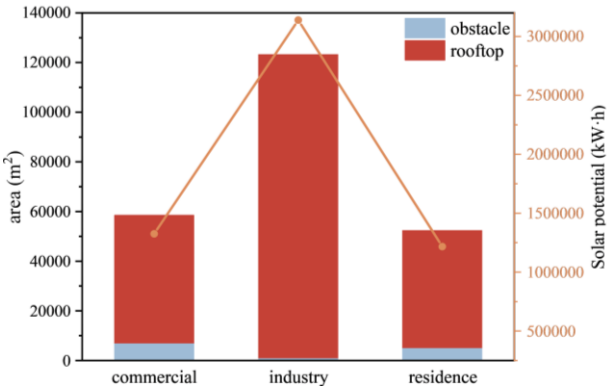

Figure 11: Calculation results of area and solar potential

Acknowledgments

This work is jointly supported by the Opening Fund of State Key Laboratory of Green Building in Western China (No. LSKF202316), the National Natural Science Foundation of China (No. 51906181), and the 2021 Construction Technology Plan Project of Hubei Province (No. 2021-83).

Conclusion

Taking Wuhan as an example, this paper constructed a rooftop recognition method based on deep learning. Classify according to different building uses, trained models to identify rooftops and obstacles, and explored the differences in the available area of rooftops for different building uses. Combined with the RayMan

model, the solar radiation amount is simulated and calculated to assess the solar photovoltaic potential in some areas of Wuhan. This paper is concluded as follows:

(1) After classifying and processing the three types of buildings, namely "commercial", "industry", and "residence", the results of identification through U^2-Net are relatively better. Among them, the best results are obtained by identifying the rooftops of "industry" buildings, with an $maxF_\beta$ value of 0.884 after classification.

(2) From the recognition results, the $maxF_\beta$ value recognized for "obstacle" is much smaller than that for "rooftop". After classification processing, for the "rooftop" label, $maxF_\beta$ has a maximum value of 0.884 for the identification of industrial buildings, and for the "obstacle" label, $maxF_\beta$ has a maximum value of 0.454 for the identification of commercial buildings, which means that there is a more accurate identification result for the rooftop.

(3) Based on the available area of the rooftop calculated from the identification results after classification processing, and combined with the solar irradiance results simulated by the RayMan model, the calculated solar photovoltaic potential in the region is as follows: The photovoltaic potential of commercial, industrial and residential buildings is 1325737.956 kW·h, 3138928.184 kW·h, 1217287.85 kW·h, respectively.

References

Dixit, Mayank, Kuldeep Chaurasia, and Vipul Kumar Mishra. 2021. 'Dilated-ResUnet: A novel deep learning architecture for building extraction from medium resolution multi-spectral satellite imagery', *Expert Systems with Applications*, 184.

Huang, Zhaojian, Thushini Mendis, and Shen Xu. 2019. 'Urban solar utilization potential mapping via deep learning technology: A case study of Wuhan, China', *Applied Energy*, 250: 283-91.

K, Simonyan, and Zisserman A. 2014. 'Very deep convolutional networks for large-scale image recognition'.

Liang, Jianming, Jianhua Gong, and Wenhang Li. 2018. 'Applications and impacts of Google Earth: A decadal review (2006–2016)', *ISPRS Journal of Photogrammetry and Remote Sensing*, 146: 91-107.

Liu, Nian, Junwei Han, and Ming-Hsuan Yang. 2018. 'Picanet:Learning pixel-wise contextual attention for saliency detection', *In Proceedings of the IEEE Conference on Computer Vision and Pattern Recognition*: 3089–98.

Mainzer, Kai, Sven Killinger, Russell McKenna, and Wolf Fichtner. 2017. 'Assessment of rooftop photovoltaic potentials at the urban level using publicly available geodata and image recognition techniques', *Solar Energy*, 155: 561-73.

Matzarakis, A., F. Rutz, and H. Mayer. 2010. 'Modelling radiation fluxes in simple and complex environments: basics of the RayMan model', *Int J Biometeorol*, 54: 131-9.

O, Ronneberger, Fischer P, and Brox T. 2015. 'U-Net: Convolutional networks for biomedical image segmentation'.

Qi, Feng, and Yixiang Wang. 2014. 'A new calculation method for shape coefficient of residential building using Google Earth', *Energy and Buildings*, 76: 72-80.

Qin, Xuebin, Zichen Zhang, Chenyang Huang, Masood Dehghan, Osmar R. Zaiane, and Martin Jagersand. 2020. 'U2-Net: Going Deeper with Nested U-Structure for Salient Object Detection', *Pattern Recognit*, 106.

Ren, Haoshan, Chengliang Xu, Zhenjun Ma, and Yongjun Sun. 2022. 'A novel 3D-geographic information system and deep learning integrated approach for high-accuracy building rooftop solar energy potential characterization of high-density cities', *Applied Energy*, 306.

Shi, Y., Q. Li, and X. X. Zhu. 2020. 'Building segmentation through a gated graph convolutional neural network with deep structured feature embedding', *ISPRS J Photogramm Remote Sens*, 159: 184-97.

V, Iglovikov. 2018. 'TernausNet: U-Net with VGG11 encoder pre-trained on ImageNet for

image segmentation'.

Yu, Jiafan, Zhecheng Wang, Arun Majumdar, and Ram Rajagopal. 2018. 'DeepSolar: A Machine Learning Framework to Efficiently Construct a Solar Deployment Database in the United States', *Joule*, 2: 2605-17.

Zhang, Chen, Zhixin Li, Haihua Jiang, Yongqiang Luo, and Shen Xu. 2021. 'Deep learning method for evaluating photovoltaic potential of urban land-use: A case study of Wuhan, China', *Applied Energy*, 283.

Zhang, Lu, Ju Dai, Huchuan Lu, You He, and Gang Wang. 2018. 'A bi-directional message passing model for salient object detection', *In Proceedings of the IEEE Conference on Computer Vision and Pattern Recognition*: 1741–50.

Zhong, Teng, Zhixin Zhang, Min Chen, Kai Zhang, Zixuan Zhou, Rui Zhu, Yijie Wang, Guonian Lü, and Jinyue Yan. 2021. 'A city-scale estimation of rooftop solar photovoltaic potential based on deep learning', *Applied Energy*, 298.